Device-Independent Color via Spectral Sharpening

Mark S. Drew and Graham D. Finlayson
School of Computing Science, Simon Fraser University
Vancouver, British Columbia, Canada

Abstract

Color sensors in scanners and color copiers are not colorimetric—RGB values are not a linear transformation away from device-independent XYZ tristimulus values. For a given set of targets or dyes one can readily find a best linear transform or use interpolation. However, when the possible targets are unknown, a data-independent transform is needed.

Here, we set out a very simple linear transform for forming XYZ from RGB, developed in analogy with a well-known solution for the color constancy problem in computer vision, based on using narrow-band sensors. In a scanner, we know the illuminant. Therefore the color constancy paradigm—illumination-independent colors—is not applicable. Instead, we change filters—from RGB to XYZ. The von Kries adaptation form of the color constancy solution can then apply if we can "sharpen" both the RGB sensors and the XYZ color-matching functions. Recently, we developed just such a "sharpening" basis transform: most of the sensitivity of the new possibly partly negative sensors is isolated in a particular wavelength interval. Here we "sharpen" both sensor sets; after dividing by sharpened white-spot values an inverse transform results in recovered XYZ values. Applying the method to 462 Munsell chips yields a median CIELAB error of only 3 units for two different systems.

1. Introduction

Color sensors in scanners and color copiers are not colorimetric, in the sense that when three filters are employed the resulting RGB values are not a linear transformation away from the X, Y, Z tristimulus values[1] that would be produced by integrating the color signal impinging on the optical system with CIE color-matching functions.[2] The transformation from RGB to XYZ forms the first step in developing a device-independent description of color for these devices.[3] For a given set of targets or set of dyes one can readily find the best linear transform, or else use interpolation and look-up table.[4,5,6] When possible targets are unknown, a data-independent transform is needed.[7]

Here, we set out a very simple linear transform for forming XYZ from RGB. The transform is developed in analogy with a simple solution for the color constancy problem in computer vision. The color constancy problem is concerned with the observation that the human vision system can correctly identify colors in a manner more or less independent of the incident illumination, e.g., grass looks green, and more or less the same shade of green, whether or not clouds cover the sun.

It has long been known that the color constancy problem has a simple solution provided it is possible to make observations using very narrow-band sensors. Suppose an illuminant with spectral power distribution (SPD) $E(\lambda)$ impinges on a surface with spectral reflectance function $S(\lambda)$. Then if the filter-optical system has transmission profile $r(\lambda)$ the resulting signal is,

$$R = \int_{\omega} E(\lambda)S(\lambda)r(\lambda)d\lambda \,,$$

integrating over the visible spectrum ω. If there are three color sensors $\underline{r}\,(\lambda)$, then the measured RGB values are

$$\underline{R} = \int_{\omega} E(\lambda)S(\lambda)\underline{r}(\lambda)d\lambda \qquad (1)$$

(showing vector quantities by an underscore).

The color constancy problem consists of recovering RGB values $\underline{R}$ formed under one illuminant from RGB values taken under another illuminant. The simplest model of color constancy is a "diagonal matrix transform" (DMT); in this model one simply multiplies each channel R, G, B by a different number separately. If a DMT holds then for a reference reflectance $S_W(\lambda)$, and two illuminants $E^1(\lambda)$, $E^2(\lambda)$, for the particular reflectance of interest $S(\lambda)$ one must have

$$\frac{\int_{\omega} E^1(\lambda)S(\lambda)\underline{r}(\lambda)d\lambda}{\int_{\omega} E^1(\lambda)S_w(\lambda)\underline{r}(\lambda)d\lambda} = \frac{\int_{\omega} E^2(\lambda)S(\lambda)\underline{r}(\lambda)d\lambda}{\int_{\omega} E^2(\lambda)S_w(\lambda)\underline{r}(\lambda)d\lambda} \qquad (2)$$

where here we stack together all three channels: the equation represents three separate equations, one for each channel. One can see that if sensor sensitivities $\underline{r}\,(\lambda)$ were very narrow-band, then eq. (2) would indeed hold. Eq. (2) embodies the notion of von Kries adaptation to changing illumination.

The denominators in eq. (2) are often called "white-spot" values because the reference reflectance is typically white.

In a scanner or color copier, we know the illuminant. Therefore eq. (2) is not the appropriate equation to use. However, a very similar situation obtains if we are interested in the relationship between measured RGB and tristimulus values XYZ. If we use 1931 CIE color matching functions $\bar{x}(\lambda), \bar{y}(\lambda), \bar{z}(\lambda)$, collectively denoted $\underline{x}\,(\lambda)$, then the three tristimulus values XYZ are given by

$$\underline{X} = \int_{\omega} E(\lambda)S(\lambda)\underline{x}(\lambda)d\lambda \quad (3)$$

By analogy with (2) we consider the integral ratios

$$\frac{\int_{\omega} E(\lambda)S(\lambda)\underline{r}(\lambda)d\lambda}{\int_{\omega} E(\lambda)S_w(\lambda)\underline{r}(\lambda)d\lambda} = \frac{\int_{\omega} E(\lambda)S(\lambda)\underline{x}(\lambda)d\lambda}{\int_{\omega} E(\lambda)S_w(\lambda)\underline{x}(\lambda)d\lambda} \quad (4)$$

where now the illuminant is the known scanner illuminant $E(\lambda)$. Once again we see that narrow-band sensors can help make eq.(4) hold, provided *both* $\underline{r}(\lambda)$ and $\underline{x}(\lambda)$ *are narrow-band* and also provided that they are *both narrow over the same wavelength range*.

At first, this seems to be asking too much. However, we show below that it is possible to transform the set of sensors $\underline{r}(\lambda)$ via a linear "sharpening transform" T^R into a new, sharpened set $\underline{r}^{\#}(\lambda)$.

Moreover, we can spectrally sharpen both sets of sensors $\underline{r}(\lambda)$ and $\underline{x}(\lambda)$ over the same wavelength intervals, concentrating each sensor set into three wavelength intervals, short, medium, and long wave. If the sharpening linear transformations are T^R and T^X for the sensor sets $\underline{r}(\lambda)$ and $\underline{x}(\lambda)$ respectively, then we can reasonably ask that for any surface reflectance $S(\lambda)$ we have

$$\frac{\int_{\omega} E(\lambda)S(\lambda)T^R\underline{r}(\lambda)d\lambda}{\int_{\omega} E(\lambda)S_W(\lambda)T^R\underline{r}(\lambda)d\lambda} = \frac{\int_{\omega} E(\lambda)S(\lambda)T^X\underline{x}(\lambda)d\lambda}{\int_{\omega} E(\lambda)S_W(\lambda)T^X\underline{x}(\lambda)d\lambda} \quad (5)$$

Since all quantities in (5) are known except the numerator of the right hand side, and since we shall also know T^X, then we can effectively retrieve the unknown tristimulus values XYZ (for the scanner illuminant) from the measured RGB values.

Below, in §4, we show how to further transform these recovered values into the standard tristimulus values for standard illuminant D65.[1]

But first, in §2 we show how to calculate the sharpening transforms T^R and T^X. In §3 we note that the transforms do not have to be calculated independently, and discuss a new optimization scheme for finding one transform in terms of the other. In §5 we examine how well the approximation performs for a large set of measured spectral reflectance functions for one system; §6 describes results for a different, 3-pass, system and shows how the anaysis can be applied to such systems. Finally, §7 presents conclusions.

2. Spectral Sharpening

In Ref. 8, we showed how to devise a linear transform T for forming combinations of a set of three sensor functions $\underline{r}(\lambda)$ that are as narrow-band as possible in a particular wavelength interval. In contrast to previous work on this problem[9], we do not insist that sensors be all positive, and our approach is analytic.

Suppose we wish to sharpen over a wavelength interval, a subset of ω. Let ϕ be all wavelengths in ω *excluding* the sharpening interval. Suppose we form a linear combination of the three sensors, $\underline{r}(\lambda)^t\underline{c}$, with coefficient vector $\underline{c}$. Here a t superscript denotes a transpose, so we are taking a dot-product of $\underline{c}$ with $\underline{r}(\lambda)$. Then we wish to choose $\underline{c}$ so as to minimize the least-squares optimization integral

$$min\ \tau_1 = \int_{\phi} [\underline{r}(\lambda)^t\underline{c}]^2 d\lambda \quad (6)$$

However, normalization is important: the best solution of (6) is $\underline{c} \equiv 0$. Therefore we impose a normalization condition by augmenting the optimization equation with a Lagrange multiplier term:

$$min\ \tau = \tau_1 + \mu\tau_2, \tau_2 = \int_{\omega} [\underline{r}(\lambda)^t\underline{c}]^2 d\lambda - 1 \quad (7)$$

The Euler equation for this problem results from taking the derivative with respect to $\underline{c}$:

$$\int_{\phi} \underline{r}(\lambda)(\underline{r}(\lambda)^t\underline{c})d\lambda + \mu\left[\int_{\omega} \underline{r}(\lambda)(\underline{r}(\lambda)^t\underline{c})d\lambda\right] = \underline{0} \quad (8)$$

The normalization constraint is recovered by taking the derivative with respect to the Lagrange multiplier μ. Then one must solve eq. (8) subject to the constraint holding.

Define the 3×3 matrix $M(\alpha) = \int_{\alpha} \underline{r}(\lambda)\underline{r}(\lambda)^t d(\lambda)$; then (8) becomes

$$M(\phi)\underline{c} = \mu M(\omega)\underline{c} \quad (9)$$

Thus the solution for the set of coefficient vectors $\underline{c}$ amounts to an eigenvalue problem

$$[M(\omega)]^{-1}M(\phi)\underline{c} = -\mu\underline{c} \quad (10)$$

There are three solutions: we choose the eigenvector which minimizes τ. The calculation must be repeated for each of three wavelength intervals. We note in Ref. 8 that both the eigenvalues and the eigenvectors of the above equation are necessarily real-valued.

Making a choice of three separate wavelength intervals, we arrive at three different coefficient vectors $\underline{c}$. Collecting these together, we have a 3×3 sharpening matrix T. Here we adopt the sharpening intervals used in Ref. 8: 400-480, 510-550, 580-650nm. Integrals are approximated by summation over spectral samples sampled every 10nm. The visible spectrum is 400-700nm. In Figure 1(a) we show the original, unsharpened CIE functions $\underline{x}(\lambda)$ and the sharpened set of sensors $\underline{x}^{\#}(\lambda)$. The relationship between them is

$$\underline{x}^{\#}(\lambda) = T^X\underline{x}(\lambda),$$

$$T^X = \begin{pmatrix} 0.50713 & -0.17050 & -0.08209 \\ -0.37580 & 0.55150 & 0.04542 \\ 0.02809 & -0.03359 & 0.26364 \end{pmatrix} \quad (11)$$

Here, $\underline{x}(\lambda)$ is a 3×3 matrix comprised of the three CIE color-matching functions. In Figure 1 (a) the unsharpened functions $\underline{x}(\lambda)$ are normalized for display.

As well, we show in Figure 1 (b) how another sharpening transform T^R affects a typical set of CCD sensor response functions $\underline{r}(\lambda)$. Here we use the response vectors for a Sony DXC151 camera with infrared filter. These sensitivities are similar to the scanner sensitivities shown in Ref. 4. In Figure1 (c) the two sharpened sets $\underline{x}^{\#}(\lambda)$ and $\underline{r}^{\#}(\lambda)$ are displayed for comparison. Every curve has norm 1.

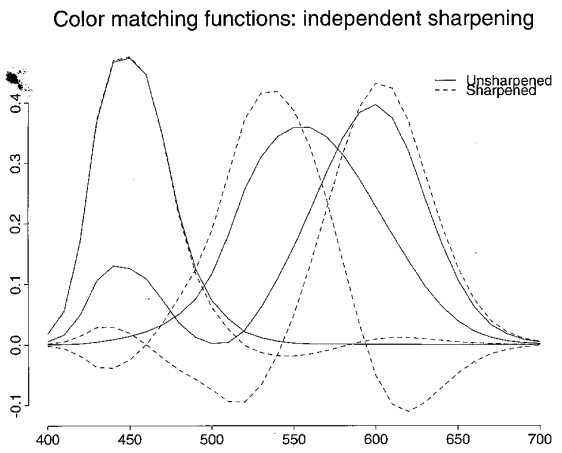

(a)

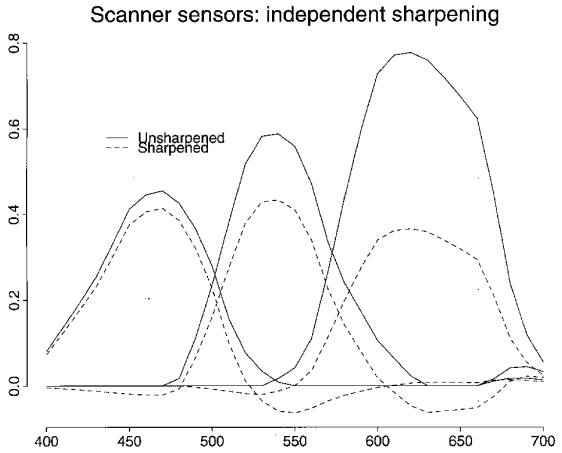

(b)

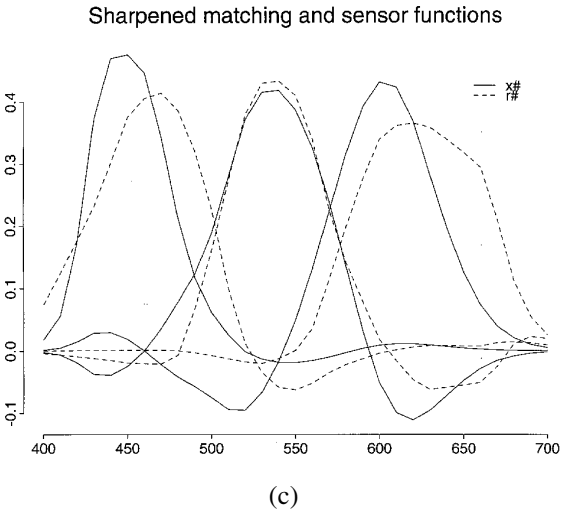

(c)

Figure 1. (a) Sharpening of $\bar{x}(\lambda), \bar{y}(\lambda), \bar{z}(\lambda)$ curves. (b) Sharpening of RGB sensor curves. (c) Comparison of sharpened curves $\underline{x}^{\#}(\lambda)$ and $\underline{r}^{\#}(\lambda)$.

Since the two sets of sensors $\underline{x}(\lambda)$ and $\underline{r}(\lambda)$ are sharpened similarly, we could put the sharpening transforms T^X and T^R into eq. (5) and hope to do well. However, first we consider below how the spectral sharpening paradigm may be altered in the present case, where two sets of sensors must be simultaneously sharpened.

3. Relative Spectral Sharpening

Since we wish to sharpen both sets of sensors $\underline{x}(\lambda)$ and $\underline{r}(\lambda)$ we could consider a minimization akin to (7) in which two terms τ_1 appear, one for each sensor set. However, the resulting equations are difficult to solve. Instead, we consider T^X fixed and attempt to find a set of sharpened $\underline{r}^{\#}(\lambda)$ that are *as close as possible to* the sharpened set $\underline{x}^{\#}(\lambda)$.

Therefore we add an additional term

$$\tau_3 = \int_\omega [\underline{r}(\lambda)^t \underline{c} - \underline{x}^{\#}(\lambda)]^2 d\lambda \qquad (12)$$

However, since such a term will set the normalization of $\underline{r}^{\#}(\lambda)$ we omit the term τ_2 which served to impose a normalization condition; $\underline{x}^{\#}(\lambda)$ is already normalized.

We cannot ask that (12) hold as a Lagrange multiplier term since that would imply that $\underline{r}^{\#}(\lambda)$ is simply the best projection $\underline{r}^{\#proj}(\lambda)$ of the three vectors $\underline{r}(\lambda)$ onto the space spanned by the three vectors $\underline{x}^{\#}(\lambda)$. Instead, we ask that the minimization proceed with a certain amount of τ_3 added: we ask for a sharpened set of sensors that are also close to the sharpened color-matching functions.

Therefore we minimize

$$min\ \tau = \tau_1 + \alpha\tau_3 \qquad (13)$$

The Euler equation corresponding to this problem is

$$\begin{aligned} &M(\phi)\underline{c} + \alpha M(\omega)\underline{c} = \alpha \underline{f}, \\ &\text{where } \underline{f} = \int_\omega \underline{r}(\lambda)^t x^{\#}(\lambda) d\lambda, \end{aligned} \qquad (14)$$

for the particular sharpening interval being considered. Note that as $\alpha \to \infty$ eq.(14) goes over to the equation for the projection of $\underline{r}(\lambda)$ onto $\underline{x}^{\#}(\lambda)$ (the transformed RGB sensors *closest* to the sharpened color-matching functions):

$$M(\omega)\underline{c}^{\#proj} = \underline{f}; \underline{r}^{\#proj}(\lambda) \equiv \underline{r}(\lambda)^t \underline{c}^{\#proj} \qquad (15)$$

For $\alpha \to 0$, the solution is $\underline{c}=0$. However, one can show that this solution is actually a zero-norm multiple of the sharpest possible set of sensors, that set resulting from sharpening $\underline{r}((\lambda)$ independent of $\underline{x}^{\#}(\lambda)$ using eq. (9) for set $\underline{r}(\lambda)$. Denote this "sharpest" set of sharpened sensors by $\underline{r}^{\#\#}(\lambda)$.

Hence, we find that it is possible to determine sharpened sensor sets for both $\underline{x}(\lambda)$ and $\underline{r}(\lambda)$. Therefore we may use eq.(5) to determine tristimulus values from measured RGB values as follows: precalculate the three white-spot values

$$\int_\omega E(\lambda) S_W(\lambda) T^R \underline{r}(\lambda) d\lambda$$

and

$$\int_{\omega} E(\lambda) S_W(\lambda) T^X \underline{x}(\lambda) d\lambda .$$

Assemble these values into two diagonal matrices. Now calculate the sharpened RGB values resulting from applying T^R to the measured RGB values for the image being scanned. Finally, eq.(5) states that the (non-sharpened) XYZ values result from combining the white-spot diagonal matrices with the sharpened RGB values and multiplying by the inverse of T^X.

So far, we have determined XYZ values with respect to the scanner illuminant, not with respect to the standard illuminant D65. In the next section we discuss how this deficiency may be remedied.

4. Illumination Change

The most useful XYZ values that we could produce would in fact be relative to the standard illuminant D65 rather than to the scanner illuminant. Here we must confront the problem of color constancy, since we are shifting illuminants. We can make use of the simplest model of color constancy, viz. eq.(2), to transform illuminants. Call the scanner illuminant $E_S(\lambda)$. Then for sharpened sensors eq.(2) implies that the following relation should hold:

$$\frac{\int_{\omega} E_S(\lambda) S(\lambda) T^X \underline{x}(\lambda) d\lambda}{\int_{\omega} E_S(\lambda) S_w(\lambda) T^X \underline{x}(\lambda) d\lambda} = \frac{\int_{\omega} D_{65}(\lambda) S(\lambda) T^X \underline{x}(\lambda) d\lambda}{\int_{\omega} D_{65}(\lambda) S_w(\lambda) T^X \underline{x}(\lambda) d\lambda} \tag{16}$$

We know the denominators in the above equation, and we have calculated the values of the numerator of the left hand side from the previous analysis. Therefore we can calculate the values of the numerator of the right hand side and, from the inverse of T^X, the tristimulus values XYZ relative to D65.

Combining eq. (5) with eq. (16) we arrive at a single matrix linking input RGB values with output XYZ values relative to illuminant D65. Let us denote the respective denominators on the left hand side and right hand side of eq. (5) by the diagonal matrices Λ_S^R and Λ_S^X. The diagonal matrix Λ_S^X also appears as the denominator of the left hand side of eq. (16). Denote the denominator of the right hand side of eq. (16) by Λ_D^X. Then we can combine (5) and (16) into the following form:

$$\underline{X}_D = (T^X)^{-1} (\Lambda_D^X / \Lambda_S^R) T^R \underline{R}_S, \tag{17}$$

relating RGB values $\underline{R}_S$ measured by the scanner to XYZ device-independent values $\underline{X}_D$ relative to illuminant D65.

5. Simulation Results

We carried out sharpening of $\underline{x}(\lambda)$ as in Figure 1, and also sharpened the Sony response curves $\underline{r}(\lambda)$ both independently, using eq. (9), and relative to $\underline{x}^{\#}(\lambda)$, as in eq. (14), for a number of values of α. The sharpened curves are shown in Figure 2. For large α, the curves $\underline{r}^{\#}(\lambda)$ go over to the set $\underline{r}^{\#proj}(\lambda)$. In Figure 2 we show curves $\underline{r}^{\#}(\lambda)$ for α=1.0 to 5.0 in steps of 1.0. The long-wave (red) sensors are displayed. For α=10.0, $\underline{r}^{\#}(\lambda)$ is very close to $\underline{r}^{\#proj}(\lambda)$. For very small α, $\underline{r}^{\#}(\lambda)$ is a scaled multiple of $\underline{r}^{\#\#}(\lambda)$.

To test how well eq. (17) performs in recovering XYZ values from measured RGB values, we performed a simulation using the 462 spectral reflectance functions of Munsell chips as measured by Newhall et al.[10] We used measured values for the spectral power distribution of a fluorescent light for the scanner illuminant. Values measured by a PhotoResearch PR650 Spectra-colorimeter were reduced to values every 10nm by carrying out a moving average. The fluorescent light used is shown in Figure 3. Table 1 shows the median CIE $L^*a^*b^*\Delta E$ error values obtained by sharpening $\underline{r}(\lambda)$using eq. (14) over a range of α values. Two values are shown: the first row of ΔE errors are for XYZ values relative to the scanner illuminant; the second row of ΔE errors are for XYZ values relative to standard illuminant D65.

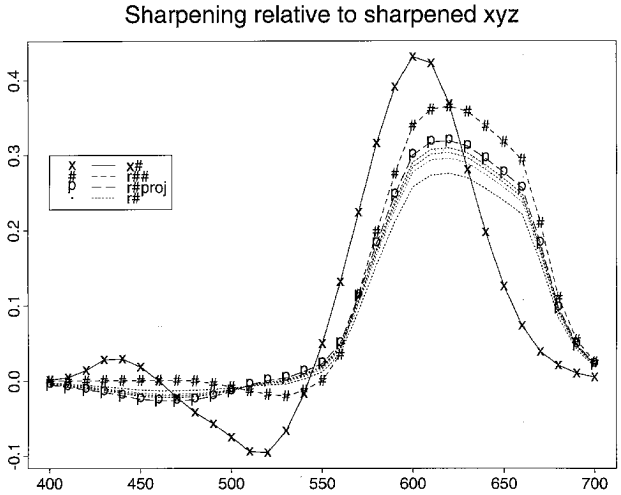

Figure 2. Relative sharpening, long wave sensor. Solid line: sharpened XYZ curve; dashed line labeled '#': sharpest RGB sensor; line labeled 'p': projection of RGB sensors onto sharpened SYZ curves; dotted lines: sharpened RGB sensors relative to sharpened XYZ curves for α from 1.0 to 5.0.

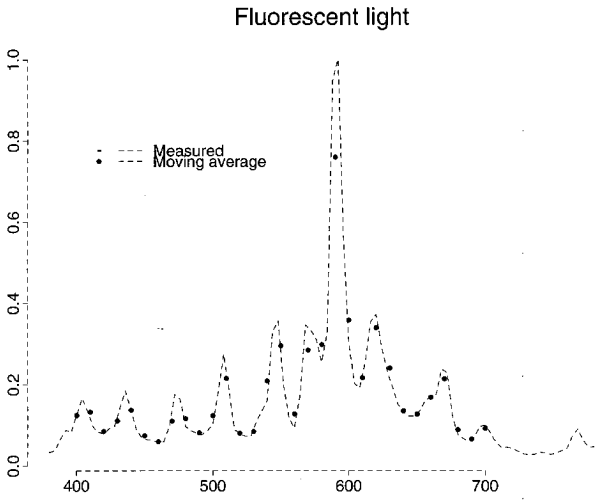

Figure 3. Scanner illuminant, reduced to 10nm samples by moving averages.

Table 1. Median CIELAB ΔE values relative to scanner illuminant and relative to illuminant D65 for several values of α for 462 Munsell samples.

α	0.0	1.0	3.0	5.0	10.0
ΔE_S	6.02	2.91	3.01	3.00	2.99
ΔE_D	6.05	3.50	3.57	3.48	3.32

The value α=0 corresponds to $\underline{r}^{\#}(\lambda)=\underline{r}^{\#\#}(\lambda)$, the sensor set $\underline{r}(\lambda)$ sharpened independently. This is the sharpest set that can be formed from $\underline{r}(\lambda)$. The value $\alpha \to \infty$ (α=10.0 in the table) corresponds to $\underline{r}^{\#}(\lambda)=\underline{r}^{\#proj}(\lambda)$, the sensor set found by projecting onto the space of sharpened XYZ curves $\underline{x}^{\#}(\lambda)$.

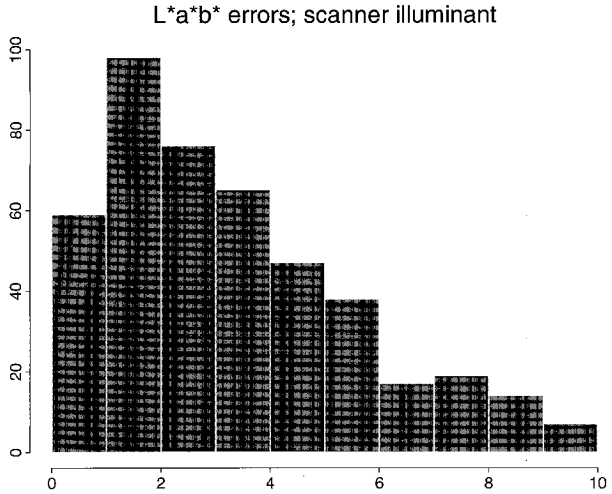

(a)

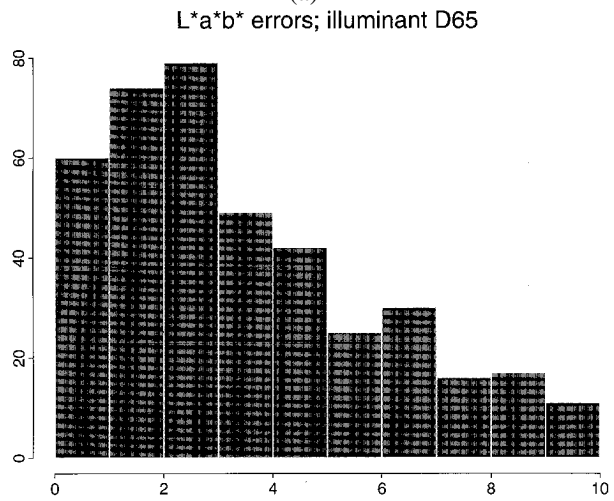

(b)

Figure 4. CIELAB errors for recovered XYZ values, relative to standard illuminant D65.

As can be seen, the sharpened set $\underline{r}^{\#proj}(\lambda)$ produces the best results (smallest ΔE) relative to illuminant D65. However, note that this may not be true in general for any set of reflectance data. Figure 4 shows a histogram, using $\underline{r}^{\#}(\lambda)=\underline{r}^{\#\text{proj}}(\lambda)$, of the second type of ΔE value.

Figure 5 shows the recovered XYZ values relative to illuminant D65, compared to the correct XYZ values, for the 462 Munsell test patches. Here, XYZ triples are projected into the chromaticity plane *x=X/(X+Y+Z),y=Y/(X+Y+Z)*. The area inside the spectrum locus delineates the convex hull of actual *xy*-values for the Munsell patches. Error bars are shown extending from correct values to those recovered by the algorithm presented here.

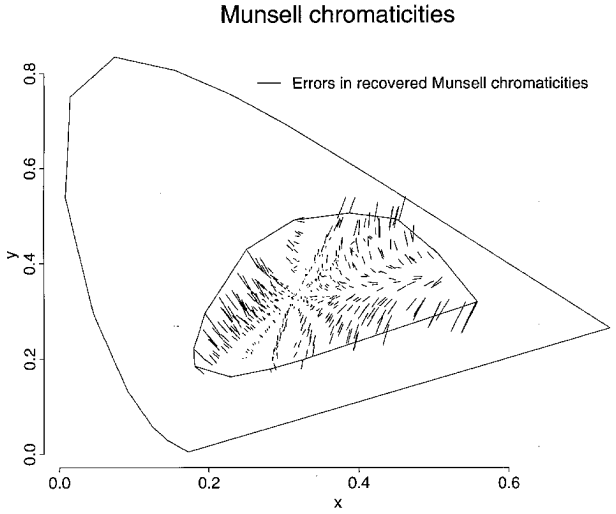

Figure 5. Chromaticities, relative to D65: Spectrum locus, plus correct chromaticities of Munsell patches; error bars to chromaticities of recovered XYZ values.

The ΔE values in Table 1 above are smaller than, or at most comparable to, values reported by Roetling[11] and Hung.[6] They report average ΔE values in the range 5 to 10 when input samples differing from the training set are used. Here for the projected sensor set, the medians of ΔE values are 2.99 and 3.32, relative to the scanner illuminant and relative to D65, respectively. The mean errors are 4.01 and 5.08 relative to the two illuminants.

6. 3-Pass Scanner

We have so far been assuming a 1-pass scanner that uses one illuminant and three filters. Some scanners, however, are 3-pass, using three differently colored lights. E.g., the Sharp JX450 scanner in Ref. 3 is 3-pass; for this scanner data is known in terms of illuminant SPD times imaging system response including the mirror and CCD†.

For a 3-pass scanner the analysis of §3 and §4 carries through with the scanner illuminant $E_S(\lambda)$ set to unity and all the response and illuminant SPD lumped into $\underline{r}(\lambda)$. Figure 6(a) shows the three response functions $\underline{r}(\lambda)$ as well as their independently sharpened versions $\underline{r}^{\#\#}(\lambda)$.
It can be seen that these are already quite sharp.

We found in §5 that in fact the best results were obtained using $\underline{r}^{\#proj}(\lambda)$. Since here we must effectively sharpen $E_S(\lambda)\underline{r}(\lambda)$ we project onto the sharpened product $[(D65(\lambda)\underline{x}(\lambda)^{\#}]$, shown in Figure 6(b).

The results are quite comparable to those of §5 when applied to the collection of Munsell patches. For the Sharp scanner we find that the mean ΔE value, relative to illuminant D65, is 3.9, and the median value is 3.4.

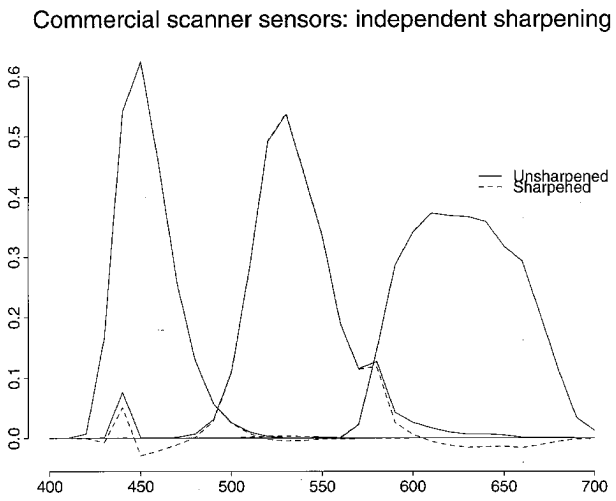

(a)

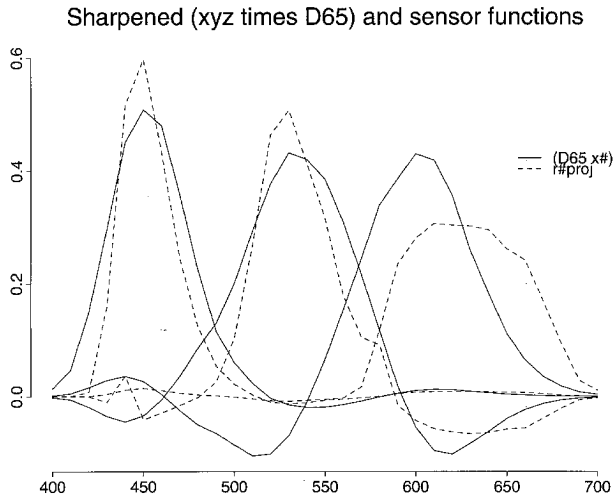

(b)

Figure 6. (a) Response functions $\underline{r}(\lambda)$ *for Sharp JX450 scanner and sharpened versions* $\underline{r}^{\#\#}(\lambda)$. *(b) Sharpened [color matching functions* $\underline{x}(\lambda)$ *times D65] and projection* $\underline{r}^{\#proj}(\lambda)$ *onto them.*

7. Conclusions

We have developed a very simple RGB→XYZ algorithm based on spectral sharpening. Adopting Wandell and Farrell's pithy phrase, we have transformed "water" into "wine."[3] The results for tests performed are good. One might ask whether it might not be simpler to just project the original sensors $\underline{r}(\lambda)$ onto the color-matching functions $\underline{x}(\lambda)$, thus forming a set of (unsharpened) projected sensors $\underline{r}^{proj}(\lambda)$, as suggested in Ref. 11. For the same conditions as in §5, we obtain quite large errors for this alternate set of colorimetric sensors.Thus a scheme such as we have proposed seems preferable. It is important to realize that the present method does not remedy the problem of metamerism; the sharpened sensors are still not a linear transformation away from human eye sensors. Nevertheless the method could guide one in designing a set of sensors with sharpened versions closest to sharpened XYZ curves. Departures from scanner linearity are another concern, but they are not corrected for here.

In general, since a large range of possible sensor sets can be sharpened sensors could be chosen on the basis of cost or convenience. Sensors need not be narrow-band to begin with; broad sensors can still be sharpened and are better, in fact, in terms of transmitting more light to the optical system.

Because of the sharpening transform one could also use more than three non-colorimetric filters that don't necessarily combine to an exact linear transformation away from XYZ curves. On the other hand, the present method does not lend itself well to dealing with fluorescent materials.

Finally, here we are dealing with only the first stage in color transformation: colorimetric matching, not appearance matching. However, the latter could be accomplished more accurately using sharpened filters.

References

† The scanner data for the Sharp JX450 (an aptly named brand for this study) is due to Brian Wandell and Joyce Farrell.

1. G. Wyszecki and W. S. Stiles. *Color Science: Concepts and Methods, Quantitative Data and Formulas*. Wiley, New York, 2nd edition, 1982.
2. J. E. Farrell, G. Dispoto, R. Motta, J. Meyer, E. J. Chichilinisky and B. A. Wandell. Sources of scanner calibration errors, In *IS&T's Eighth International Congress on Advances in Non-Impact Printing Technologies*, pages 491-495, 1992.
3. B. A. Wandell and J. E. Farrell. Water into wine: Converting scanner RGB to tristimulus XYZ. In *Device-Independent Color Imaging and Imaging Systems Integration*, pages 92-101. *SPIE* Vol. **1909**. 1993.
4. S. Suzuki, T. Kusunoki and M. Mori. Color characteristic design for color scanners. *Applied Optics*, **29**: 5187-5192, 1990.
5. P. C. Hung. Color rendition using three-dimensional interpolation. In *Imaging Applications in the Work World*, pages 111-115, *SPIE* Vol. **900**, 1988.
6. P. C. Hung, Colorimetric calibration for scanners and media. In *Proceedings of the1991 Electronic Imaging Meeting*, San Jose, CA., Feb., 1991.
7. R. E. Burger. Device Independent color scanning. In *Device-Independent Color Imaging and Imaging Systems Integration*, pages 70-74. *SPIE* Vol **1909**, 1993.
8. G. D. Finlayson. M. S. Drew and B. V. Funt. Spectral sharpening: sensor transformations for improved color constancy. *J. Opt. Soc. Am. A*, **11**:1553-1563, 1994.
9. M. L. Pearson and J. A. Yule. Transformations of color mixture functions without negative portions. *J. Color and Appearance*, **2**:30-35, 1973.
10. S. M. Newhall, D. Nickerson, and D. B. Judd. Final report of the OSA subcommittee o n the spacing of the munsell colors. *J. Opt. Soc. Am.*, **33**:385-418, 1943.
11. P. G. Roetling, J. E. Stinehour and M. S. Maltz. Color characterization of a scanner. In *IS&T's Seventh International Congress on Advances in Non-Impact Printing Technologies*, pages 433-440, 1991.

published previously in the IS&T 1994 Color Imaging Conference Proceedings, page 121